

# Investigations of the galaxies of the LCV

Dimitrios Papachistopoulos

March 20, 2023

## Abstract

---

## 1 The Galaxies in the Local Cosmological Volume (LCV)

The Catalogue of Neighbouring Galaxies (Karachentsev, Igor D. and Makarov et al. 2013[2]) and its updated version from the “Catalog & Atlas of the LV galaxies” databas[1] are used to extract the K-band luminosities, the types of the galaxies, the mass within the Holmberg radius (M26), the Hydrogen masses of the galaxies ( $M_{HI}$ ) and the SFRs based on integrated H and far-ultraviolet (FUV) measurments for galaxies within a distance of  $\approx 11$  Mpc. The SFR values contain limit flags, which we exclude from our present analysis. This gives a sample of 793 galaxies from 1248. From the remaing galaxies we have

Measurment	Number of Galaxies
Hydrogen-Mass	643
M26	643
K-band lum.	789
Type	793
H $\alpha$ -S	566
FUV-SFR	688

The K-band values are converted to the total Stellar Masses of each galaxy according to the mass-to-light ratio of 0.6 ([4]), and the  $M_{HI}$  can be converted to the total mass of the gas of the galaxy using the equation  $M_g = 1.33 M_{HI}$

The total SFR of each galaxy can be calculated by

$$SFR_o = \frac{SFR_{FUV} + SFR_{Ha}}{2}$$

if both  $SFR_{H\alpha}, SFR_{FUV}$  measurments are available. If only one only one of them is given, then the SFR is equal to the given SFR value

$$SFR_o = SFR_i, \text{ if } SFR_j = 0, i \neq j, i, j = SFR_{FUV}, SFR_{Ha}$$

The condition  $SFR_o \geq 10^{-3} M_{\odot} yr^{-1}$  leaves 579 galaxies. This condition is applied due to the reasons given in the P. Kroupa, M. Haslbauer, I. Banik, S. T. Nagesh and J. Pflamm-Altenburg et al. 2020 [3]

## 2 Types of galaxies

Using the dataset of 1248 galaxies, do before using the condition and removing the galaxies with the flags, the below histograms can be plotted.

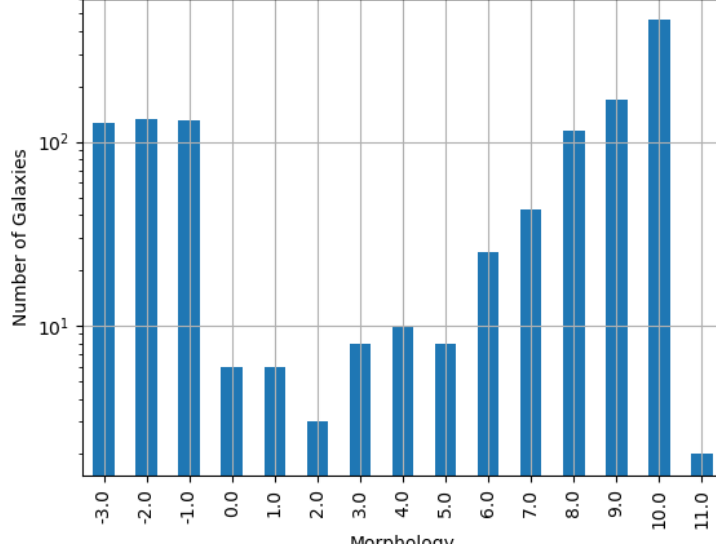


Figure 1: The classification by de Vaucouleurs et al. (1991) is used for the morphology of the galaxies

Most of the galaxies in the LCV are Higly Irregular galaxies followed by lenticular galaxies

Out of the 1248 galaxies the 1022 are dwarf galaxies

Most dwarf galaxies have low brightness and are irregulars followed by Dwarf spheroidal.

## 3 Calculation of the normalization constant

According to P. Kroupa et al. 2020 current star formation rates of galaxies can be described by the 'delayed- $\tau$ ' mode as

$$SFR_{0,del} = \frac{A_{del}xe^{-x}}{\tau}, \text{ where } x = \frac{t_{sf}}{\tau} \quad (1)$$

$\tau$  is the star formation time-scale and  $t_{sf}$  is the real time of star formation in a given galaxy

The average SFR is

$$\overline{SFR}_{del} = \frac{A_{del}}{t_{sf}} [1 - (1+x)e^{-x}] \quad (2)$$

and can also be defined by the present day stellar mass

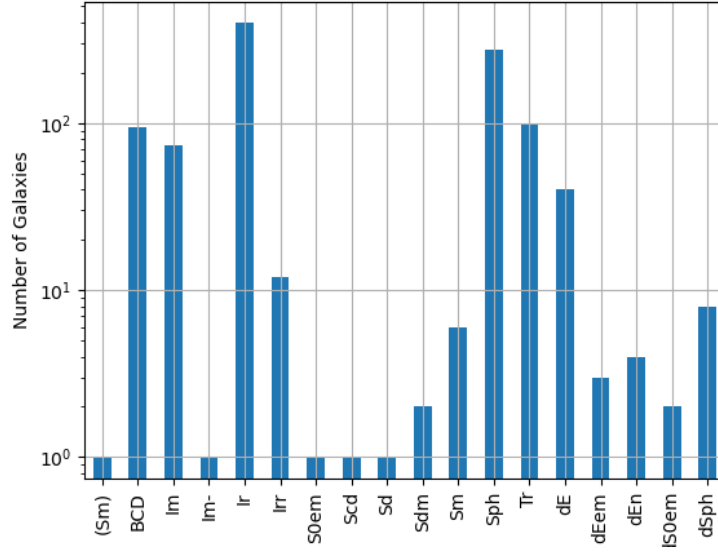


Figure 2: Dwarf galaxy morphology

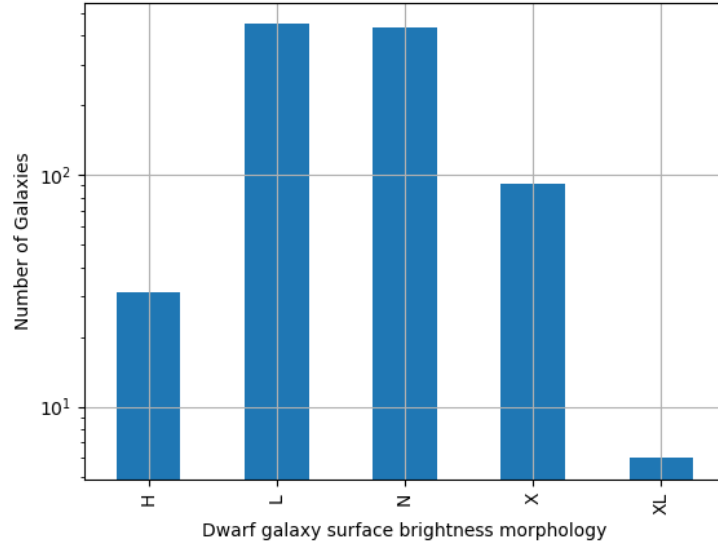


Figure 3: Dwarf galaxy surface brightness morphology, where: H = high; N = normal; L = low; X = extremely low.

$$\overline{SFR} = \frac{\zeta M_*}{t_{sf}} \quad (3)$$

where  $\zeta$  accommodates for mass-loss through stella evolution and  $\zeta \approx 1.3$

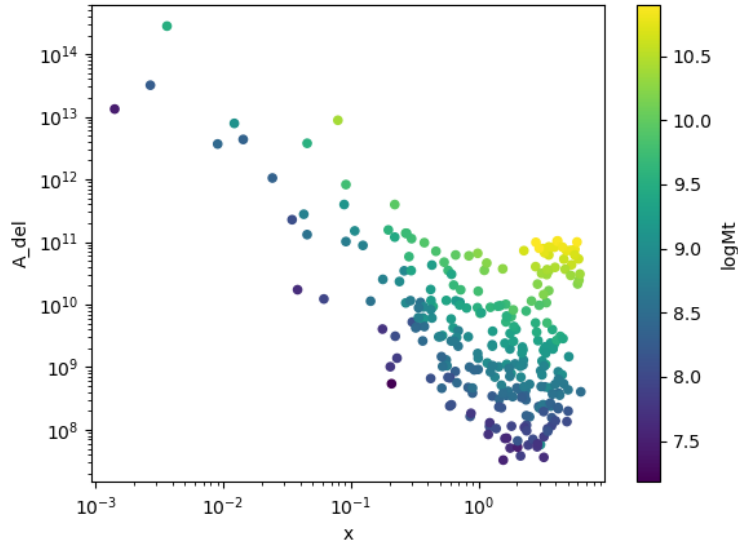
### 3.1 Constant $t_{sf}$

The observed ages of galactic discs are  $t_{sf} \approx 12$  Gyr (e.g. Knox, Hawkins & Hamblly 1999), so assuming an approximation of  $t_{sf} = 12.5$  Gyr, the  $\overline{SFR}_{del}$  can be calculated, from the equation (??). After that the equation of ratio

$$\frac{\overline{SFR}_{del}}{\overline{SFR}_{0,del}} = \frac{e^x - x - 1}{x^2} \quad (4)$$

can be solved numerically for  $x$  and using the equations (??) and (??) the  $A_{del}$  and  $\tau$  of each galaxy are found

	x	tau	A_del
count	550.000000	5.500000e+02	5.500000e+02
mean	1.762321	1.126908e+11	2.600301e+12
std	1.388768	1.067717e+12	4.456457e+13
min	0.000559	2.198306e+09	2.477977e+07
50%	1.513139	8.260984e+09	6.446495e+08
max	5.686198	2.237735e+13	1.005083e+15



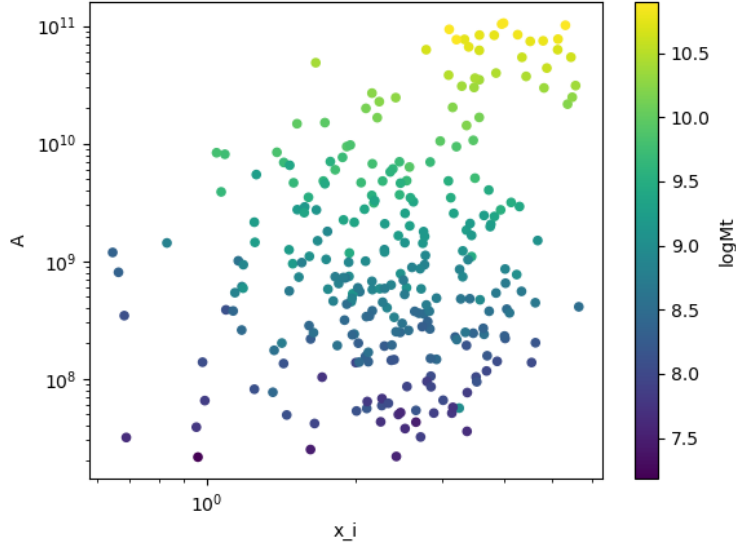
### 3.2 Constant $\tau$

Assuming for an constant  $\tau = 3.5$  Gyr, we cannot use the same  $\overline{SFR}$  and ratio. Using the equations (??) and (??)

$$\frac{\overline{SFR_{del}}}{SFR_{0,del}} = \frac{e^x - x - 1}{x^2} \Leftrightarrow \frac{e^x - x - 1}{x} = \frac{\zeta M_*}{SFR \cdot \tau}$$

and  $x$  and  $A_{del}$  can be calculated numerically.

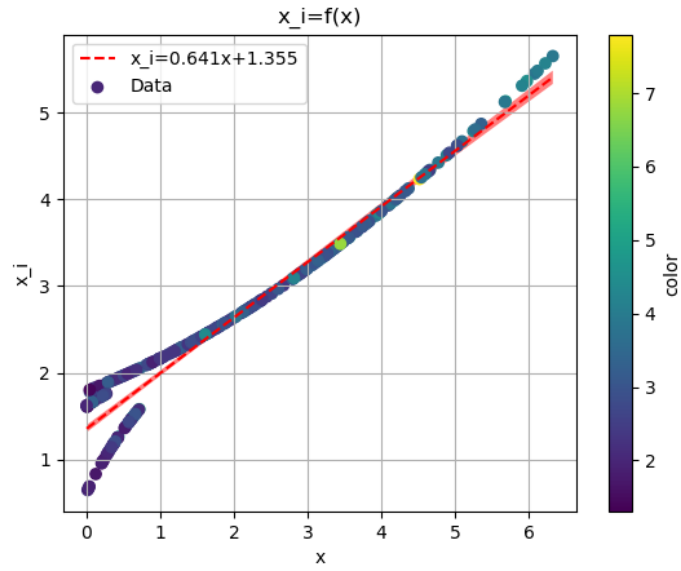
	A	tsf	x_i
count	5.500000e+02	5.500000e+02	550.000000
mean	4.192335e+09	8.727310e+09	2.493517
std	1.432226e+10	3.097809e+09	0.885088
min	9.870027e+06	2.323533e+09	0.663867
25%	6.466448e+07	6.441713e+09	1.840489
50%	2.234694e+08	8.383763e+09	2.395361
75%	1.034826e+09	1.077179e+10	3.077654
max	1.057699e+11	1.796414e+10	5.132611



Comparing the two different results for  $x$ , we see that the  $x_i$  from the second solution has a lower  $\sigma$

	x	x_i
count	550.000000	550.000000
mean	1.762321	2.493517
std	1.388768	0.885088
min	0.000559	0.663867
25%	0.558532	1.840489
50%	1.513139	2.395361
75%	2.789068	3.077654
max	5.686198	5.132611

The  $x_i$  results are more inline with the expected values from Kroupa et al. 2020  $2.7 < x < 3.4$



The galaxies with low  $x$  and  $x_i$ , have a lower color index ( $\langle B - V \rangle$ ) than galaxies with higher  $x$ , which means that they are younger galaxies, as expected by the  $x$  values. For example, if  $x$  has a value of 1  $\Leftrightarrow x_i = 2$  then

`./graphs/log_A_del-log_A.png`

The correlation between the 2 different  $x$  is good with an R-squared of 94%

### 3.2.1 TODO DO sigma clipping for x to see if the x's are in agreement with the theoritical values

## 4 Mass relations

The below graphs show the correlation that the masses of the galaxies have. To consider a correlation good we need a  $R^2 > 70\%$



Figure 4: Stellar Mass - Mass within Holmberg radius:  $R^2 = 0.8$

,

,

## 5 Calculate the gas depletion timescale $\tau_g$

The gas depletion timescale  $\tau_g$  measures the time taken by a galaxy to exhaust its gas content  $M_g$  given the current SFR (Pflamm-Altenburg & Kroupa 2009).

$$\tau_g = \frac{M_g}{\dot{M}_*} = \frac{M_g}{SFR}$$

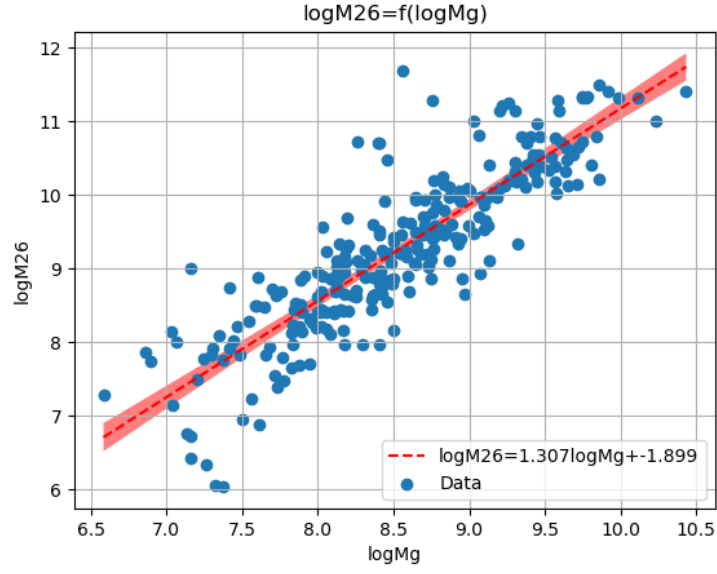


Figure 5: Gas Mass - Mass within Holmberg radius:  $R^2 = 0.77$

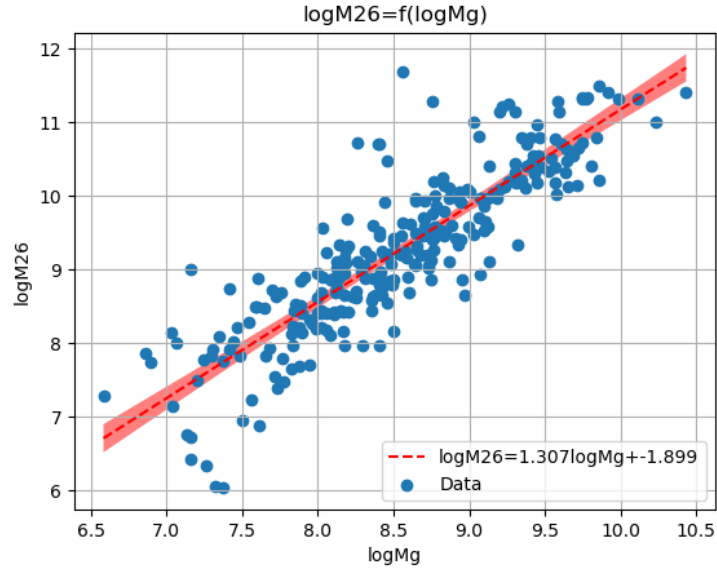


Figure 6: Gas Mass/Hydrogen Mass - Mass within Holmberg radius:  $R^2 = 0.77$



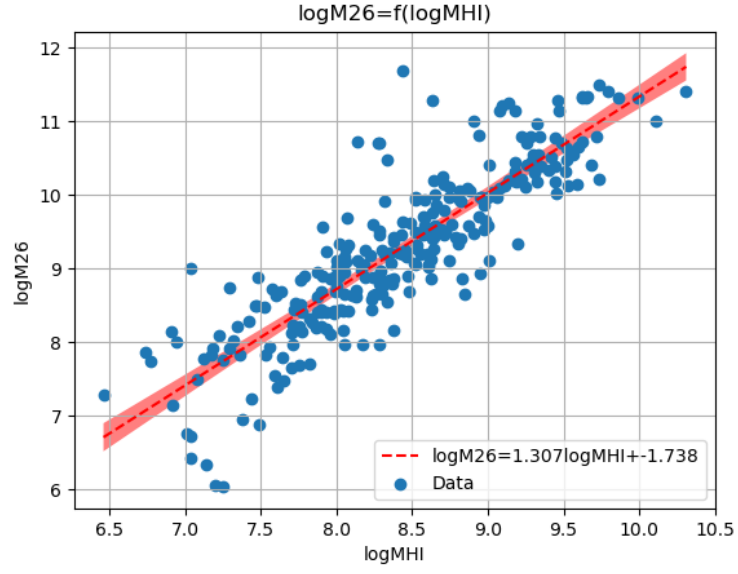


Figure 7: Gas Mass/Hydrogen Mass - Mass within Holmberg radius:  $R^2 = 0.77$

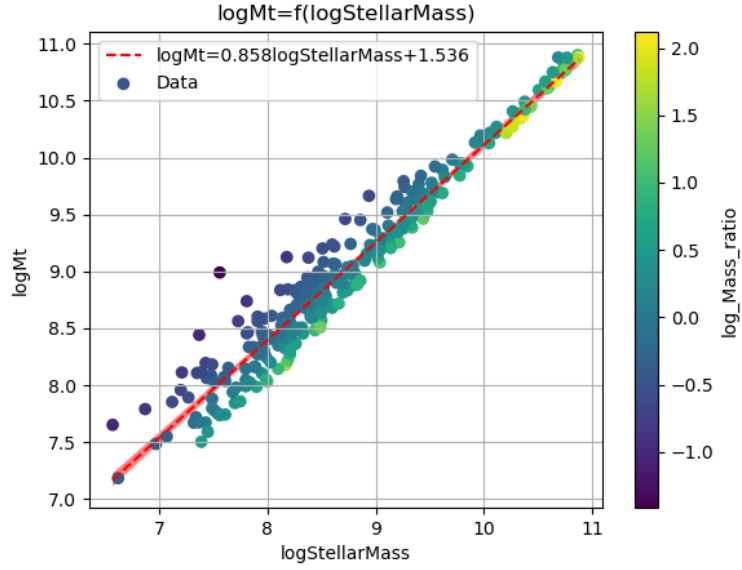


Figure 8: Total Mass - Stellar Mass:  $R^2 = 0.93$

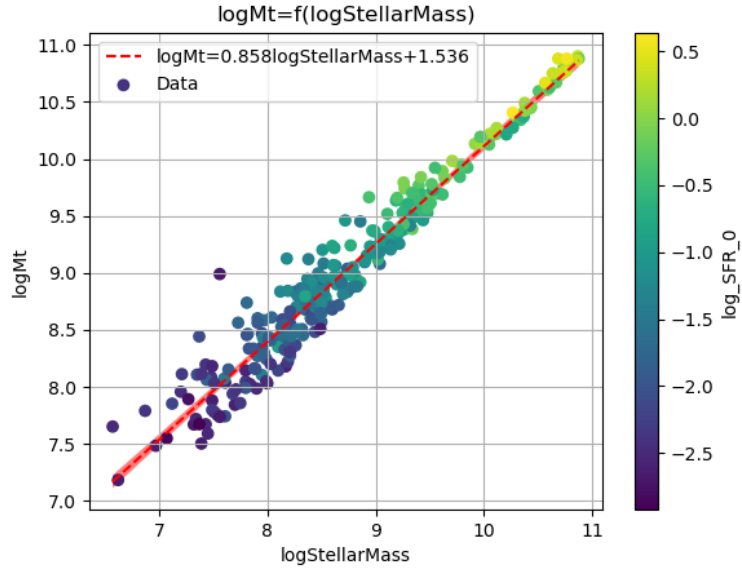


Figure 9: Total Mass - Stellar Mass:  $R^2 = 0.93$

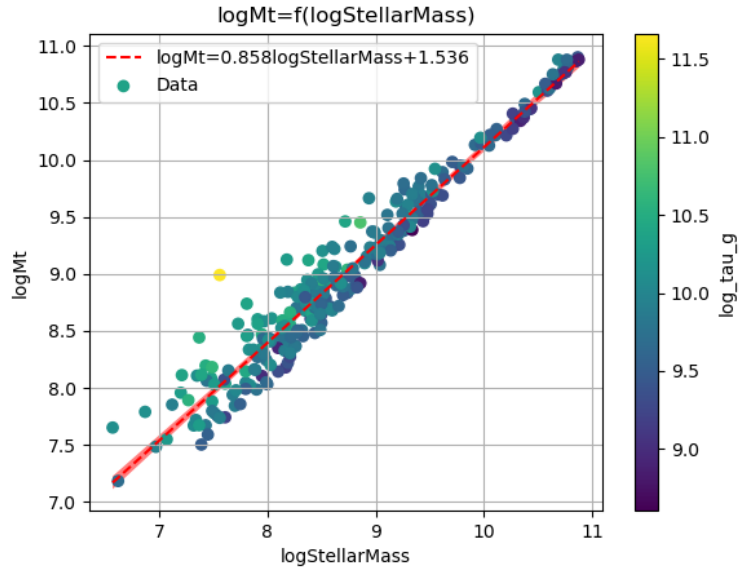


Figure 10: Total Mass - Stellar Mass:  $R^2 = 0.93$

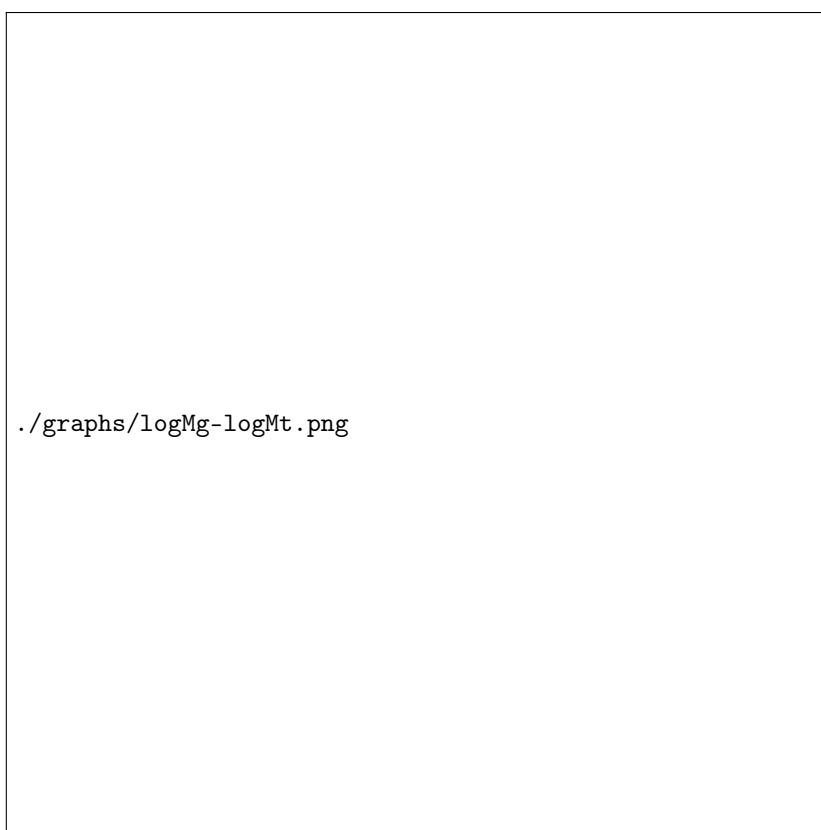


Figure 11: Total Mass - Gas Mass/Hydrogen Mass:  $R^2 = 0.87$

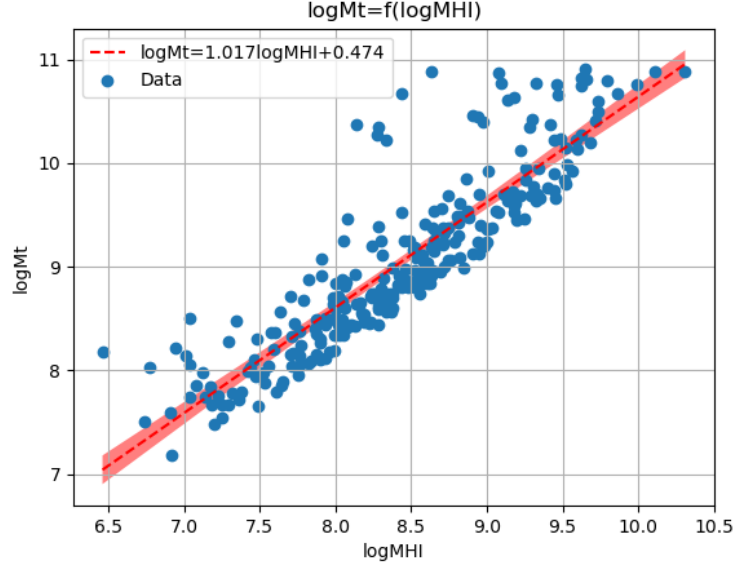


Figure 12: Total Mass - Gas Mass/Hydrogen Mass:  $R^2 = 0.87$

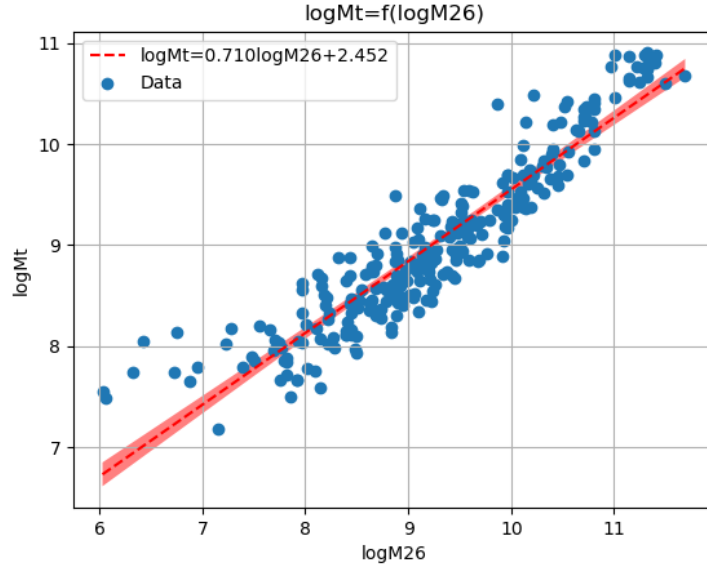


Figure 13: Total Mass - Mass within Holmberg radius:  $R^2 = 0.85$

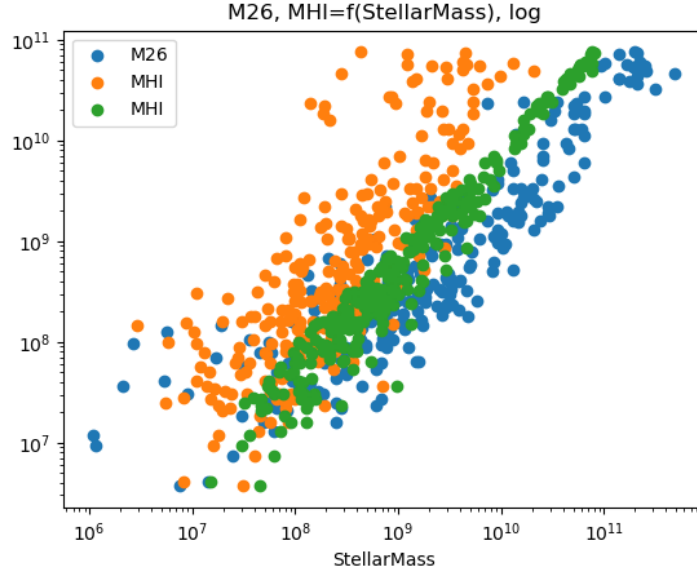


Figure 14: Stellar Mass - Mass within Holmberg radius - Hydrogen Mass - Total Mass

## References

- [1] *Catalog of the LV Galaxies*. <https://www.sao.ru/lv/lvgdb/tables.php>. (Visited on 03/13/2023).
- [2] Igor D. Karachentsev, Dmitry I. Makarov, and Elena I. Kaisina. “UPDATED NEARBY GALAXY CATALOG”. In: *AJ* 145.4 (Mar. 2013), p. 101. ISSN: 0004-6256, 1538-3881. DOI: 10.1088/0004-6256/145/4/101. (Visited on 03/13/2023).
- [3] P Kroupa et al. “Constraints on the Star Formation Histories of Galaxies in the Local Cosmological Volume”. In: *Monthly Notices of the Royal Astronomical Society* 497.1 (Sept. 2020), pp. 37–43. ISSN: 0035-8711. DOI: 10.1093/mnras/staa1851. (Visited on 03/13/2023).
- [4] Federico Lelli, Stacy S. McGaugh, and James M. Schombert. “SPARC: MASS MODELS FOR 175 DISK GALAXIES WITH SPITZER PHOTOMETRY AND ACCURATE ROTATION CURVES”. In: *AJ* 152.6 (Nov. 2016), p. 157. ISSN: 1538-3881. DOI: 10.3847/0004-6256/152/6/157. (Visited on 03/13/2023).